45th AIAA/ASME/ASCE/AHS/ASC Structures, Structural Dynamics & Materials Conference
19 - 22 April 2004, Palm Springs, California

AIAA 2004-1722

Comparison of Morphing Wing Strategies Based Upon Aircraft Performance Impacts

Shiv P. Joshi* and Zeb Tidwell†
NextGen Aeronautics, Inc., Torrance, CA, 90505

William A. Crossley‡
Purdue University, West Lafayette, IN 47907

and

Sekaripuram Ramakrishnan§
HyPerComp, Inc., Westlake Village, CA, 91362

Conventional aircraft are designed for a specific mission and/or set of performance requirements. These requirements often cause the performance for certain mission segments to be compromised because of fixed wing geometry. While some devices, such as flaps, have been used to augment the wing geometry, new materials are being developed that could allow significant wing morphing capability. This paper demonstrates the impact of a morphing wing on aircraft performance and provides a method to compare various morphing strategies.

Nomenclature

c	=	chord
D	=	drag
L	=	lift
LO	=	lift off
n	=	gravity load factor
T	=	thrust
V	=	velocity
W	=	aircraft weight

I. Introduction

Advances in smart structures and active materials during the last decade may yield significant changes from the way aircraft are presently designed.[1] These technologies may provide new ways of changing an aircraft's geometry while in flight, and several of these technologies have been demonstrated in experimental programs.[2] DARPA's recently initiated Morphing Aircraft Structures (MAS) program[3] has a goal of obtaining significant wing planform geometry changes during flight utilizing advanced actuators and devices. This program plans to include a flight-traceable wind tunnel demonstration and may lead to a flight demonstration of an aircraft with a morphing wing.

Significant geometric changes of an aircraft's wing during flight may permit efficient performance during disparate mission roles, or allow new multi-role missions not possible with a fixed-geometry aircraft. Current aircraft use conventional actuators and mechanisms to vary wing sweep for flight in different speed regimes, and to extend flaps during landing and takeoff to change wing area and camber. More advanced actuators using smart materials and adaptive structures are envisioned that could change many more geometric parameters during flight.

* Principle Engineer, 2780 Skypark Dr, Suite 400, and Senior Member AIAA.
† Senior Engineer, 2780 Skypark Dr, Suite 400, Senior Member AIAA.
‡ Associate Professor, School of Aeronautics and Astronautics, 315 N Grant St., Senior Member AIAA.
§ CFD Manager, 312555 Cedar Valley Dr, Suite 327, Senior Member AIAA.

For example, a morphing aircraft wing could be capable of changing wing area, aspect ratio, and taper ratio, which all allow the planform to change. Additionally, altering camber, thickness or twist could change the cross-section of the wing. Some geometry changes may be more useful than others, and different missions may warrant different geometric changes. Further, designers of a morphing wing must consider the various mechanization strategies available to bring about the geometry changes. These strategies may couple changes of geometry and/or limit the range of the wing's shape change; for example, a swing-wing strategy like the F-14 changes both sweep and aspect ratio, but these are coupled – the change in the aspect ratio is a direct function of the change in sweep.

The purpose of this effort is to demonstrate how various types of morphing can positively impact aircraft performance metrics and to provide a means in which different morphing strategies can be compared. Identification of the morphing strategies that demonstrate the most "morphing potential" will be an important task for designers of aircraft with morphing wings.

II. Scope and Methods of Approach

Because the goal of a morphing aircraft is to obtain near-optimal performance for several dissimilar mission roles, a wide set of performance points describing flight conditions that an aircraft might encounter during a multi-role mission provides a basis for comparison of morphing approaches and strategies. For this investigation 11 flight conditions representing various aircraft mission segments were used; these are summarized in Table 1.

Table 1: Point performance flight conditions and performance metrics.

Mission segment	Altitude	Velocity / Mach number	Performance metric
Takeoff	sea level	$V = 0$ to V_{LO}	Minimize time to accelerate $\frac{0.7 V_{LO} W}{32.2 (T_{available} - D)_{0.7V_{LO}}}$ [s]
Climb1	sea level	$V_{\text{best ROC}}$	Maximize rate of climb $\frac{V(T_{available} - D)}{W}$ [ft/s]
Climb2	30,000 ft	$V_{\text{best ROC}}$	Maximize rate of climb $\frac{V(T_{available} - D)}{W}$ [ft/s]
Cruise1	sea level	$V_{\text{best range}}$	Maximize range factor $\frac{V/1.69}{c}\frac{L}{D}$ [nm]
Cruise2	30,000 ft	$V_{\text{best range}}$	Maximize range factor $\frac{V/1.69}{c}\frac{L}{D}$ [nm]
Cruise3	60,000 ft	$V_{\text{best range}}$	Maximize range factor $\frac{V/1.69}{c}\frac{L}{D}$ [nm]
Acceleration	30,000 ft	$M = 0.5$	Maximize acceleration $\frac{T_{available} - D}{W/32.2}$ [ft/s^2]
Dash	30,000 ft	$V_{\max}$	Maximize $V_{\max}$ [ft/s]
Endurance	60,000 ft	$V_{\text{best endurance}}$	Maximize endurance factor $\frac{1}{c}\frac{L}{D}$ [hr]
Instantaneous turn	sea level	Corner speed	Maximize turn rate $\frac{32.2\sqrt{n^2 - 1}}{V}\frac{180}{\pi}$ [deg/s]
Sustained turn	60,000 ft	$V_{\text{best turn rate}}$	Maximize turn rate $\frac{32.2\sqrt{n^2 - 1}}{V}\frac{180}{\pi}$ [deg/s]

All of these flight conditions assume US Standard Atmosphere conditions. The performance metric listed indicates the quantity to be maximized or minimized to represent the "optimal" performance for the corresponding flight condition. For the performance points corresponding to takeoff and acceleration, the velocities are specified; takeoff begins from V = 0, acceleration is measured from a specified flight Mach number (M=0.5). The velocities are computed for the remaining performance points; for example, the best range velocity of the aircraft depends upon the wing planform.

In the traditional approach to design a fixed geometry aircraft, these 11 performance points might be used to develop a constraint diagram or linked together in a design mission for which an aircraft would be sized. Using either of these approaches results in a "compromise" geometry that allows the aircraft to fly at all of these flight conditions, but the performance of the aircraft at each condition is likely sub-optimal. An aircraft with a morphing wing, however, is not limited to single compromise planform; the ability to change the wing planform should allow nearly optimal performance for a collection of flight conditions than the fixed geometry aircraft.

A graphical presentation using a "radar plot" or a "spider plot" provides a way to examine the impact that a morphing wing will have on an aircraft's performance for each of the 11 flight conditions. In this spider plot concept, each axis of the plot represents the performance metric associated with each flight condition. The outer radius of the spider plot indicates the "best possible performance" for each flight condition. The performance of various wing morphing strategies can be compared by superposing plots on this spider plot format. Figure 1 presents the basic concept of this performance spider plot.

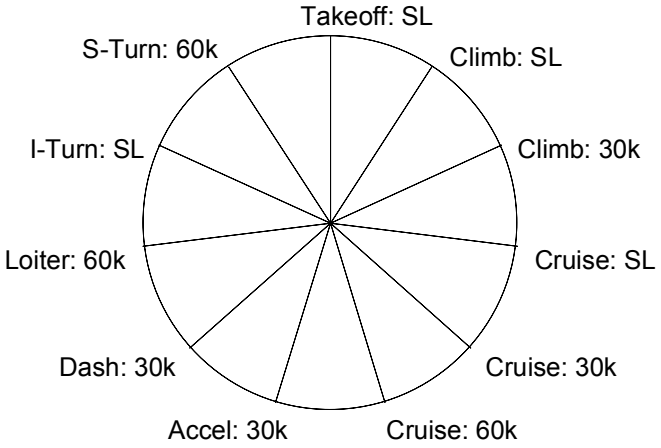

Figure 1: Performance spider plot format.

Table 1 includes basic formulae to predict values of the performance metrics (time to accelerate, rate of climb, etc.) of an aircraft. In order to calculate these performance metrics, the basic aircraft performance estimation followed approaches from aircraft design and performance textbooks of Raymer[4], Shevell[5], and Anderson[6]. These methods included a parasite drag build up, a compressibility drag estimation, an engine model for thrust as a function of Mach number and altitude, a 2-D airfoil to 3-D wing lift curve correction, and a semi-empirical estimation of Oswald's efficiency factor to allow induced drag calculations.

Following the ideas of the DARPA Morphing Aircraft Structures (MAS) program, which calls for a flight-traceable wind tunnel test of a morphing wing, the BQM-34 Firebee unmanned target drone aircraft is a promising baseline aircraft for investigating the impact of a morphing wing. The Firebee's half wingspan is about 6.5 feet, which would fit in most medium to large size wind tunnel facilities; so a wind tunnel test could examine a full scale wing. Additionally, the Firebee is constructed with an easily removable wing, which might allow for the airframe to be re-fitted with a morphing wing. Because the Firebee makes a promising baseline aircraft, the geometry of the Firebee's fuselage, blended nacelle, vertical tail and horizontal tail are used throughout this study.

To begin the study, the outer radius of the spider plot must be generated. The idea is to represent the best possible flight performance for each of the 11 flight conditions. The approach followed here was to assume that all parameters describing the wing planform are independent of each other. For this work, the wing area, S, the wingspan, b, the taper ratio, λ, and the quarter-chord sweep, Λ, are used to represent the wing planform. From these four values, the aspect ratio, root, tip and mean aerodynamic chords, and the leading edge sweep can be computed. Then, determining the best possible performance takes the form of an optimization problem: minimize or maximize the performance metric by varying the four planform variables. Without upper and lower limits on the variables or

some other set of constraints to bound the design space the optimization problem is unbounded. For instance, wingspan may become unreasonably large in an effort to increase the wing aspect ratio to values of 50 and higher. Two approaches were chosen to address this issue.

The first approach is to simply place bounds on the geometry of the wing. Table 2 presents these limits. An axial parameter, X, is used to restrict the distance between the most forward leading edge point and the most aft trailing edge point (Figure 2). The minimum wing area limit is based on a desired maximum wing loading (W/S=100 psf) and vehicle weight (W=3000 lb). The maximum wing area limit is then calculated based on the maximum percent area change (233%) of the morphing concepts developed by NextGen. The wing span limits were set to as a relative bound based on the span of the Firebee. Also, the maximum wing span limit was restricted to allow a full scale model tested at NASA Langley's TDT wind tunnel. The taper ratio is allowed to vary from a realistic triangular platform (λ=0.05) to an untapered planform. The final constraint was the wing sweep which was allowed to vary between 0 and 60 degrees.

Table 2: Limit values for geometry constrained problems.

Variable	Lower bound	Upper bound
X [ft]	none	10
S [ft^2]	30	70
b [ft]	5.0	20
λ	0.05	1.00
Λ [deg]	0	60

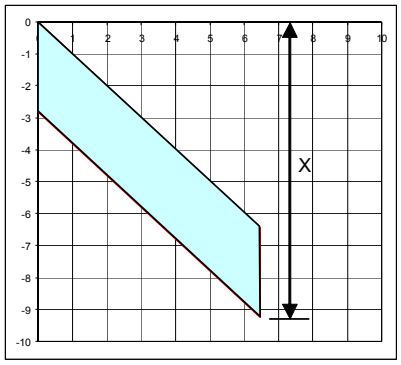

Figure 2: Typical wing with geometry constraint.

The second approach uses a wing weight estimation to constrain the upper bound of the wing area and span (Table 3). The upper bound for the predicted wing weight, W, was defined as 10% of the gross takeoff weight of the baseline Firebee vehicle (2350 lbs). This is a reasonable weight constraint compared to the actual Firebee wing weight of 165 lbs.

Table 3: Limit values for weight constrained problems.

Variable	Lower bound	Upper bound
W [lb]	none	235
S [ft^2]	30	none
b [ft]	5.0	none
λ	0.05	1.00
Λ [deg]	0	60

The performance metric for each of the 11 flight conditions was then optimized with Excel's Solver add-in (generalized reduced gradient) using the wing planform design variables (wing area, wingspan, taper ratio, and sweep) and constraints (geometry or weight method). The results were used to define the outer radius of the spider plots (optimal performance). A similar performance optimization of various NextGen morphing planform concepts was then performed. For each concept, the wing planform variables were coupled and/or restricted based on the morphing strategy used.

An additional trade study was performed to determine the benefit of a morphing airfoil with a fixed wing planform. HyPerComp performed a two-dimensional CFD airfoil optimization for the defined 11 flight conditions. The airfoil geometry was defined with 11 parameters (a nose radius plus 10 control points for NURBS). The flow parameters used were Mach number, Reynolds number, and angle of attack. Figure 3 shows the interface of HyPerComp's airfoil optimizer.

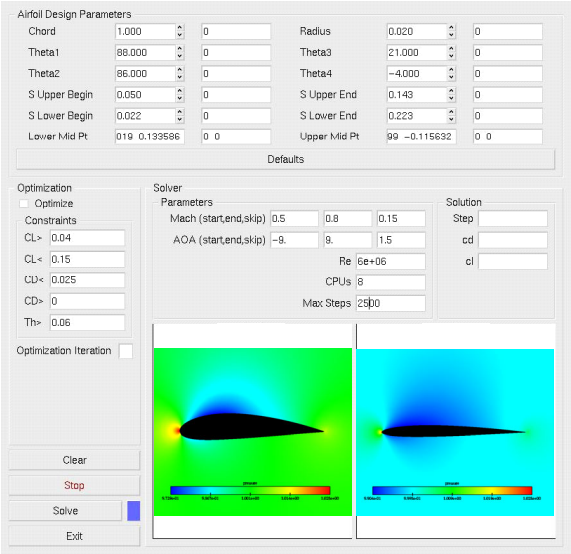

Figure 3: Airfoil optimization interface.

The algorithm uses automatic meshing and a high fidelity flow solver until the optimal metric parameter is achieved using a gradient-based optimization scheme. The flow solver uses the full Navier-Stokes equation, an upwind wind TVD scheme, a one equation turbulent model, and an unstructured mesh based bookkeeping approach. Results are summarized in Table 4. The airfoil data of the Firebee wing was then replaced with the optimal airfoil data for each flight condition and the vehicle performance was recalculated.

Table 4: CFD airfoil optimization results.

	1	2	3	4	5	6	7	8	9	10	11
Mission Segment	Takeoff	Climb		Cruise Range			Accel.	Dash	Loiter Endure.	Instant Turn	Sustained Turn
Altitude	SL	SL	30K ft.	SL	30K ft.	60K ft.	30K ft.	30K ft.	60K ft.	SL	60K ft.
Mach Number	0.2	0.433	0.7	0.3	0.6	0.7	0.3	0.6	0.7	0.3	0.7
Reynolds No. ($\times 10^6$)	4.36	10.04	6.53	6.95	5.60	1.68	2.80	5.60	1.68	6.95	1.68
Parameter	$(C_L)_{max}$	C_{D0}	C_{D0}	L/D	L/D	L/D	D (C_{D0})	C_{D0}	L/D	$(C_L)_{max}$	L/D
Airfoil 01	1.7880	0.00640	0.01560	108.24	77.01	17.47	0.01668	0.01040	17.47	1.8594	17.47
Airfoil 02	1.6090	0.00540	0.00880	92.52	53.52	23.33	0.01482	0.00900	23.33	1.4057	23.33
Airfoil 04	1.4000	0.00680	0.01765	109.06	73.84	15.83	0.01602	0.01480	15.83	1.7800	15.83
Airfoil 05	1.6284	0.00630	0.01095	105.83	80.95	20.91	0.01590	0.01050	20.91	1.6871	20.91
Airfoil 08	1.9324	0.00745	0.02105	111.18	83.04	unsteady	0.00986	0.01890	unsteady	unsteady	unsteady
Airfoil 09	1.6090	0.00540	0.00880	92.52	53.52	23.33	0.01482	0.00900	23.33	1.4057	23.33
Airfoil 11	1.7880	0.00640	0.01560	108.24	77.01	17.47	0.01668	0.01040	17.47	1.8594	17.47
Airfoil 13	1.7380	0.00631	0.01067	101.21	58.58	27.35	0.01566	0.01060	27.35		27.35
NACA0014	1.4830	0.00570	0.00870	81.31	49.30	12.36	0.01553	0.00910	12.36		12.36

Optimal airfoil for mission segment

III. Conclusions

As a result, morphing strategies can be compared using the "spider plots". An example spider plot appears in Figure 4. In this plot, the fixed geometry Firebee appears as the inner most area; the Firebee was designed as a high-speed target drone, so it is quite good at climbing and high-speed flight. The Firebee is also quite poor at high-altitudes, especially in its ability to perform a sustained turn at 60,000 ft above sea level; this should be expected, because the aircraft was not designed with this capability in mind. Next on the plot, moving outward from the center, is a plot representing an aircraft with the Firebee's wing planform, but the airfoil can morph to a shape better suited to each performance point flight condition. This airfoil morphing provides some notable improvements in performance, particularly in the phases of flight for which the original Firebee is not well suited. The outermost shaded area represents the performance of a Firebee sized aircraft with a wing capable of telescoping, chord extension and variable sweep. This planform morphing significantly improves the aircraft performance over that provided by morphing the airfoil alone.

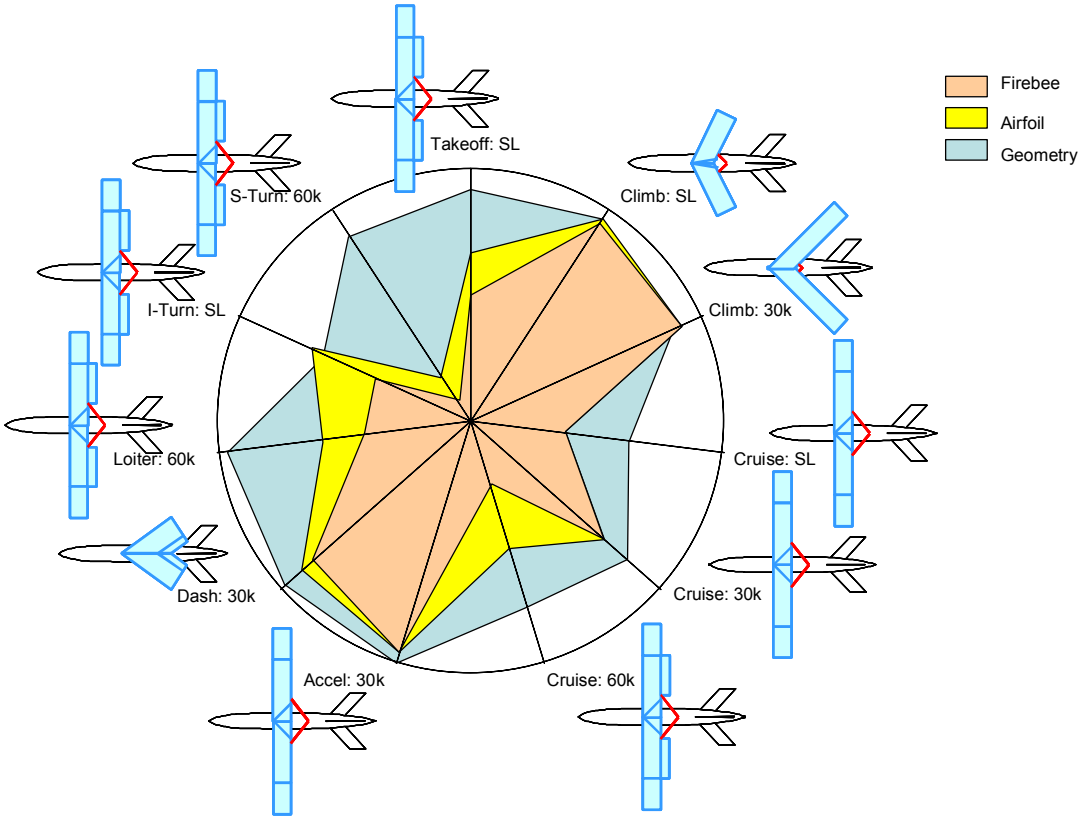

Figure 4: Spider plot comparing predicted performance of the fixed-geometry Firebee, a morphing airfoil Firebee and a morphing planform Firebee.

A summation of the non-dimensionalized performance values allows a quantitative comparison of various morphing strategies; the highest cumulative value suggests the best morphing strategy. This comparison assumes that each performance point is equally important, like a weighted-sum approach to a multiobjective optimization problem. The selection of the most promising morphing strategies is possible using this measure.

Acknowledgments

The work documented in this paper was performed under a DARPA/AFRL contract to a team lead by NextGen Aeronautics entitled, "Next Generation Morphing Aircraft Structures (N-MAS)," F33615-02-C-3257. The DARPA Program Manager is Dr. Terrance A. Weisshaar and the AFRL Technical Agent is Dr. Brian Sanders.

References

[1]Wlezien, R. W., Horner, G. C., McGowan, A. R., Padula, S. L., Scott, M. A., Silcox, R. H., and Simpson, J. O., "The Aircraft Morphing Program," AIAA 98-1927, 39th AIAA/ASME/ASCE/AHS/ASC Structures, Structural Dynamics, and Materials Conference, Apr. 1998.

[2]Kudva, J., Martin, C., Scherer, L., Jardine, A., McGowan, A., Lake, R., Sendeckyj, G., and Sanders, B., "Overview of the DARPA/USAF/NASA Smart Wing Program," Proceedings *of the SPIE Smart Structures and Materials Conference 1999*, Vol. 3674, International Society for Optical Engineering, Newport Beach, CA, 1999, pp. 230-236.

[3] Wall, R., "Darpa Eyes Materials for 'Morphing' Aircraft," *Aviation Week and Space Technology*, April 8, 2002.

[4] Raymer, D. P., *Aircraft Design: A Conceptual Approach*, 3rd edition, AIAA, Reston, VA, 1999.

[5] Shevell, R. S., *Fundamentals of Flight*, 2nd edition, Prentice-Hall, Englewood Cliffs, NJ, 1989.

[6] Anderson, Jr., J. D., *Aircraft Performance and Design*, WCB/McGraw Hill, Boston, 1999.